Monthly Notices
of the
ROYAL ASTRONOMICAL SOCIETY

Mon. Not. R. Astron. Soc. **412,** 2689–2694 (2011) doi:10.1111/j.1365-2966.2010.18103.x

The optical light curve of the Large Magellanic Cloud pulsar B0540−69 in 2009

S. Gradari,[1,2]★ M. Barbieri,[1] C. Barbieri,[1] G. Naletto,[3,4] E. Verroi,[1,3] T. Occhipinti,[1,3] P. Zoccarato,[1,2] C. Germanà,[1] L. Zampieri[1] and A. Possenti[5]

[1]*Department of Astronomy, University of Padova, Vicolo dell'Osservatorio 3, Padova 35122, Italy*
[2]*CISAS, University of Padova, Padova 35100, Italy*
[3]*Department of Information Engineering, University of Padova, Via Gradenigo 6/B, Padova 35131, Italy*
[4]*CNR-IFN UOS Padova LUXOR, Padova, Padova 35100, Italy*
[5]*INAF – Osservatorio Astronomico di Cagliari, loc. Poggio dei Pini, strada 54, Capoterra 09012, Italy*

Accepted 2010 November 24. Received 2010 November 24; in original form 2010 July 8

ABSTRACT

This paper reports a detailed analysis of the optical light curve of PSR B0540−69, the second brightest pulsar in the visible band, obtained in 2009 (January 18 and 20, and December 14, 15, 16 and 18) with the very high speed photon-counting photometer Iqueye mounted at the ESO 3.6-m New Technology Telescope in La Silla (Chile). The optical light curve derived by Iqueye shows a double structure in the main peak, with a rising edge steeper than the trailing edge. The double peak can be fitted by two Gaussians with the same height and full width at half-maximum of 13.3 and 15.5 ms, respectively. Our new values of spin frequencies allow us to extend by 3.5 yr the time interval over which a reliable estimate of frequency first and second derivatives can be performed. A discussion of implications for the braking index and age of the pulsar is presented. A value of $n = 2.087 \pm 0.007$ for the overall braking index from 1987 to 2009 is derived. The braking index corrected age is confirmed at around 1700 yr.

Key words: instrumentation: photometers – techniques: photometric – pulsars: general – pulsars: individual: PSR B0540−69.

1 INTRODUCTION

B0540−69 is a 50-ms optical pulsar in the Large Magellanic Cloud, the second brightest in the optical band after the Crab pulsar. It has been observed in recent years with a variety of imaging and spectroscopic instruments on the ground as well as space telescopes [Serafimovich et al. 2004; De Luca et al. 2007; Mignani et al. 2010; all references are based on *Hubble Space Telescope* (*HST*) data]. However, the number of published optical light curves is fairly small, and all amount to data obtained more than 10 years ago. The first published light curve was obtained by Middleditch & Pennypacker (1985) and Middleditch, Pennypacker & Burns (1987) using the 4-m and 1.5-m telescopes at Cerro Tololo. Then, Gouiffes, Finley & Ögelman (1992) derived a second light curve from data taken with the ESO 3.6-m telescope in the interval 1989 January–1991 April. Boyd et al. (1995) obtained a third light curve with the High Speed Photometer (HSP) on board the *HST*. All light within the HSP sensitivity band from 160 to 700 nm was used, observing the pulsar for 1 h on 1993 August 26 through a 0.65-arcsec diaphragm. The sample time was 300 μs. The HSP light curve was consistent with the shape seen by Middleditch et al. (1987) and Gouiffes et al. (1992), and showed with clarity a double peak structure. This light curve was compared to those obtained by several hard X-ray instruments by De Plaa, Kuiper & Hermsen (2003), who fitted the pulse shape with a double Gaussian curve. A fourth curve, from data obtained in 1994 May at the ESO 3.6-m telescope, was inserted by Mignani et al. (1998) in a paper about the pulsar PSR B1509−58. Subsequently, Deeter, Nagase & Boynton (1999) published a light curve based on data originally taken by Manchester & Peterson (1989) at the 4-m Anglo-Australian Telescope over the period 1986 July 14 to 1988 June 16. Finally, Ulmer et al. (1999) published a light curve obtained at CTIO in 1996 November, and suspected a strong phase difference between optical and X-ray data. All those optical pulse shapes are consistent with the radio one (Manchester et al. 1993) and with those observed in the X- and gamma-ray domains (e.g. Deeter et al. 1999; Mineo et al. 1999; De Plaa et al. 2003; Campana et al. 2008).

We observed the pulsar at the ESO New Technology Telescope (NTT) with our very high speed photometer Iqueye [the prototype of a 'quantum' photometer for the European Extremely Large Telescope (E-ELT); Dravins et al. 2005] in 2009 January and December. Our optical light curve is therefore the first derived from data acquired since 1996. In Section 2 we describe the instrument and

★E-mail: serena.gradari@unipd.it

Table 1. Geodetic and geocentric Cartesian coordinates of the NTT (top of the roof, doors open, dome still).

Longitude (°)	Latitude (°)	Elevation (m)	X (m)	Y (m)	Z (m)
−70.733746	−29.258913	2424.09	+1838193.1	−5258983.2	−3100153.8

observations. The results from these observations are expounded in Section 3, and their implications on braking index and age are discussed in Section 4.

2 THE IQUEYE SINGLE PHOTON-COUNTING PHOTOMETER

For a description of the scientific motivations of Iqueye and of its optomechanical characteristics see Barbieri et al. (2009) and Naletto et al. (2009), and references therein. In essence, Iqueye has been conceived as a precursor to a quantum photometer for the future 42-m E-ELT (see Dravins et al. 2005), aiming to perform not only high-speed photometry, but also measurements of the statistics in the photon arrival times and intensity interferometry (Hanbury Brown 1974). Iqueye is a conceptually simple fixed-aperture photometer which collects the light within a field of view (FOV) of a few arcseconds around the target object. It is mounted at the Nasmyth focus of the 3.6-m ESO NTT. A holed folding mirror at 45° on the NTT focal plane brings a 1-arcmin field around the star under investigation to the field acquisition TV camera. The light from the target object instead passes through the central hole and is collected by a collimating refracting system. Two filter wheels located in the parallel beam after the first lens allow the selection of different filters and polarizers. Then the light reaches a focusing system which (de)magnifies the telescope image by a 1/3.25 factor. On this intermediate focal plane, one out of three pinholes (200, 300 and 500 μm diameter) can be inserted. These pinholes act as field stops, and their sizes allow the selection of three different FOVs (3.5, 5.2 and 8.7 arcsec diameter). After the pinhole, the light impinges on a pyramid having four reflecting surfaces and whose tip coincides with the centre of the shadow of the secondary mirror. The pyramid splits the telescope pupil in four equal portions, and sends the light from each subpupil along four perpendicular arms. Along each arm, the subpupil light is first collimated and then refocused by a suitable system, further (de)magnifying the image by an additional 1/3.5 factor. Each subbeam is then focused on a single photon avalanche photodiode (SPAD) operated in Geiger mode. The quantum efficiency of the silicon SPADs extends from the blue to the near-infrared, with a peak sensitivity of 55 per cent at 550 nm. When used without filter, as in the present case, the overall efficiency of Iqueye (SPAD+telescope+atmosphere) at the zenith is approximately 33 per cent. The dark counts of the temperature-controlled detectors are very low, varying from 30 to 50 count s^{-1} for each individual unit. The SPAD circular sensitive area of 100 μm diameter nominally defines a 5.8-arcsec FOV. Therefore, the smallest pinhole acts as the actual field stop at 3.4 arcsec. This pinhole can be selected when it is necessary to reduce as much as possible the background around the target, e.g. when observing a pulsar embedded in a nebula, as in the present case. The optical solution of splitting the beam by a pyramid in four subbeams was dictated by the need to overcome as much as possible the dead time intrinsic to the SPAD (75 ns), in order to give to Iqueye the largest possible dynamic range. In other scientific applications (e.g. intensity interferometry), having four independent detectors allows cross-correlation of the counts from each subaperture. The pulses produced by the SPADs, which have an intrinsic time jitter of the order of 35 ps, are sent to a time to digital converter (TDC) board which has a nominal resolution of 24.4 ps. Considering also the other possible noise sources, the nominal accuracy of the photon arrival time determination is of the order of 100 ps or better. An external rubidium oscillator provides the reference frequency to the TDC board. The board acquires also a pulse per second (PPS) from a global positioning system (GPS) receiver, used to remove the rubidium frequency drift and to put the internal detection times on the UTC scale. Taking into account all error factors, the final overall precision of each time tag in the UTC scale is approximately 450 ps, maintained throughout the duration of the observations. In order to take care as well as is feasible of the rotation of the NTT building, the GPS antenna was mounted on the top of the dome, at the centre of one of the sliding doors (about 3 m away from the dome rotation axis). The signal was brought to the receiver by a high-quality, length compensated cable. The geodetic and geocentric Cartesian coordinates of the antenna, in the WGS94 reference system, are given in Table 1. These coordinates have been translated to the intersection of the optical and elevation axes using the construction drawings of the enclosure; taking into account the rotation of the dome, the actual precision is estimated better than 2 m. This uncertainty on the position of the detector reflects in a maximum uncertainty on the barycentred times of arrival of the photons of 7 ns but does not influence significantly the values either of the period or of the phases, as we have also tested by changing the position of values by several tens of metres.

The user interface, developed as a Java multitasking code, controls each subsystem (e.g. the mechanisms), performs the data acquisition and storage, provides some real time monitoring of the data acquisition and also provides tools for a quick look statistical analysis of the data. Each arrival time is recorded on the storage device which has a total capacity of approximately 2 TB. The data being stored in a mass memory device, all the data can be analysed in post-processing: this allows, for example, sorting of the collected time tags in arbitrarily long time bins still preserving the original data. Between the January and December runs, some improvements were made to the instrument (Barbieri et al. 2010; Naletto et al. 2010), in particular the addition of a fifth SPAD to acquire the signal from the sky.

3 OBSERVATIONS AND ANALYSIS

The observations were obtained through 3.5 or 5.2 arcsec diaphragms, without filters (maximum sensitivity around 550 nm, bandwidth at half-maximum approximately 300 nm). The observation log is provided in Table 2. The columns UTC and MJD = Modified Julian Date = JD – 240 0000.5 provide values of time and date at mid-counting period referred to the barycentre of the Solar system in TCB units (see later for the adopted procedure).

The procedure we routinely follow at the telescope to centre faint pulsating objects is to bin the arrival times in convenient time bins, e.g. 1/20 of the expected period, so that standard time-series analysis algorithms can be applied to single out the frequencies in the signal. After few minutes of trying in a given position, a slightly different one is tested until the position giving the best

Table 2. Log of the observations of Iqueye at the NTT.

Date	UTC (hh mm ss)	MJD (mid-exposure time) (d)	Observation duration (s)	Diaphragm diameter (arcsec)	Detected photons
2009 January 18	05 11 10.0	54849.21665	5994	3.5	8304 630
2009 January 20	04 03 19.0	54851.16190	5874	5.2	17 775 124
2009 December 14	07 27 59.9	55179.31111	3600	3.5	21 917 637
2009 December 15	02 42 00.0	55180.11250	3600	3.5	10 767 547
2009 December 16	01 39 59.6	55181.06944	3000	5.2	13 896 153
2009 December 18	02 30 00.3	55183.10417	3600	3.5	10 262 179

Table 3. Periods and frequencies of PSR B0540−69 determined with Iqueye data obtained during 2009.

Date (MJD)	Period (s) and error (s)	Frequency (Hz) and error (Hz)
54849.21665	0.050 649 9745 (43.8×10^{-9})	19.743 3466 (17.1×10^{-6})
54851.16190	0.050 650 0173 (23.8×10^{-9})	19.743 3299 (9.3×10^{-6})
55179.31111	0.050 663 5498 (44.4×10^{-9})	19.738 0563 (17.3×10^{-6})
55180.11250	0.050 663 6329 (25.4×10^{-9})	19.738 0239 (9.9×10^{-6})
55181.06944	0.050 663 6715 (49.1×10^{-9})	19.738 0089 (19.1×10^{-6})
55183.10417	0.050 663 7532 (24.3×10^{-9})	19.737 9771 (9.5×10^{-6})

signal is found. Then, a long observation is started. In the case of B0540−69, the procedure converged very quickly. The power spectral density of the data was dominated by a frequency at the expected (according to the ephemerides available in the literature) value of 19.7433 Hz (period around 0.05065 s) for January's data and 19.7380 Hz (period around 0.05066 s) for December's data with a statistical significance higher than 20 standard deviations (σ) of noise; no other signal was visible above 3σ of noise in the range 0–200 Hz. In December, this standard procedure was greatly helped by the availability of a very deep finding chart, kindly provided by Mignani et al. (2010) (their fig. 1) before publication.

In order to perform the detailed analysis of the period and light curve, the arrival times of the photons are referred to the barycentre of the Solar system, by using the latest release of the Tempo2 software (Hobbs, Edwards & Manchester 2006) with the DE405 JPL Ephemerides (Standish 1998). The assumed celestial coordinates of the source are RA(2000) = $05^{\rm h}40^{\rm m}11\overset{\rm s}{.}202 \pm 0\overset{\rm s}{.}009$; Dec.(2000) = $-69^\circ 19' 54\overset{''}{.}17 \pm 0\overset{''}{.}05$ (Mignani et al. 2010), with zero proper motion (De Luca et al. 2007; Mignani et al. 2010). These values have been measured on images taken with the *HST*/Wide Field Planetary Camera 2 (WFPC2) through the F555 and F547 nm filters, and have been referred to the absolute reference frame using astrometric data of the dense Two Micron All Sky Survey (2MASS) catalogue (Skrutskie et al. 2006). Therefore, the positions of Mignani et al. (2010) are more accurate than those published by Serafimovich et al. (2004) and by Shearer et al. (1994).

We can consider the width of the peak in the signal Fourier transform, $P^2/(2\Delta t)$, where P is the period and Δt the observing time, which corresponds to a few microseconds in our cases, as the intrinsic resolution of the period. So, we took advantage of the actual much better timing performance of the instrument to determine the period with the highest possible accuracy. For this, we analysed a 3 μs wide intrinsic resolution window around the expected period in steps of 0.1–0.3 ns by means of an epoch-folding technique similar to that expounded by Leahy, Elsner & Weisskopf (1983). The spin period P was computed separately for each night, starting from the values given by Livingstone, Kaspi & Gavriil (2005) and reported to our dates including the effect of the first and second spin period derivatives. For each period, the χ^2 values against the zero hypothesis of a flat curve were calculated, obtaining a well-defined distribution peaked around the expected value. The best period was then obtained through a least-squares fit of the χ^2 distribution with a Gaussian curve. The mean value of the Gaussian is the best-fitting period. The error on this measurement was calculated starting from the Monte Carlo estimate of Leahy (1987) for sinusoidal signals and correcting it following the approach of Larsson (1996), which makes optimum usage of the full pulse shape information, or equivalently all its Fourier components. By comparing equations (4) and (5) of Larsson (1996) we see that the period error for a non-sinusoidal signal is $\sigma_{\rm P} = \sigma_{\rm P,s}/\sqrt{\sum_k k^2 A_k^2/A^2}$, where A_k are the amplitudes of the different Fourier components and $\sigma_{\rm P,s}$ is the period error if the signal were a sinusoid with the same period and with amplitude A. The accuracy of the period determination is increased taking a weighted mean of the harmonics of the signal. $\sigma_{\rm P,s}$ can be expressed using equation (6a) for sinusoidal signals in Leahy (1987), while the amplitudes A_k are determined from a Fourier component analysis of the signal. A is taken approximately equal to A_1. In Table 3 we report the results of the procedure, in terms of both the measured period P and the corresponding pulsar spin frequency ν. The quoted errors on P are determined as explained above, while those on ν are obtained by error propagation.

With our data alone, obtained over a time-span of 1 yr, we can determine the first derivative of the frequency. Using $t_0 = 55183.1042$ (MJD) as reference date in a linear fit, we obtain $\nu_0 = 19.7379712 \pm 4.83 \times 10^{-6}$ Hz and $\dot{\nu}_0 = -1.86346 \times 10^{-10} \pm 2.65 \times 10^{-13}$ Hz s^{-1}. These values are in good agreement with those available in the literature as discussed at the end of the Section 4.

The combined Iqueye light curve for all nights of 2009 January and December is shown in Fig. 1 using 50 phase bins and displayed

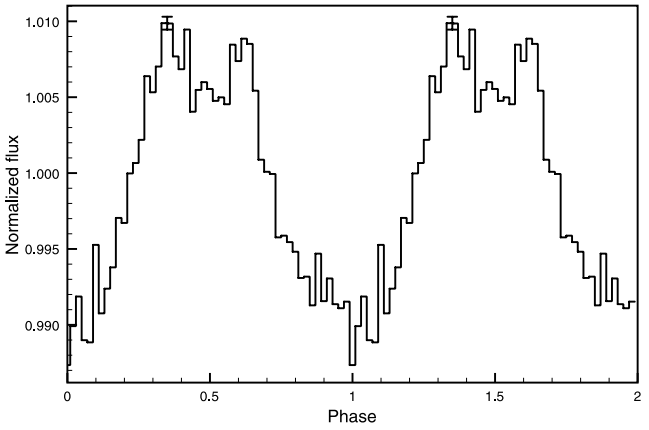

Figure 1. The overall Iqueye light curve in 2009 January and December from the individual curves weighted according to the respective χ^2 value and binned in 50 phase intervals. The counts have been normalized to the average count value during a period. For clarity the curve is shown over two cycles. The vertical bar shows the 1σ error. All light curves were shifted to match the phase of December 18.

for better visualization over two cycles. All light curves were shifted to match the phase of December 18 because of the better signal-to-noise (S/N) ratio of those data. Each curve has been weighted for the respective χ^2 value of the period determination and the alignment by minimizing the distance between the curves using again the χ^2 method.

The modulation M of our light curve, defined as

$$M = \frac{\langle c \rangle - c_{\min}}{\langle c \rangle}, \tag{1}$$

where $\langle c \rangle$ is the mean count rate in the pulse profile and $c_{\min}$ is the minimum count rate, is of the order of 1.5 per cent for the light curve obtained with Iqueye, a value similar to that shown by the light curves resulting from the published observations performed at other ground-based telescopes. Therefore, all available light curves published over the last 27 years have approximately the same modulation, and broadly show the same features, namely a main pulse with a total duty cycle of about 45 per cent and complex structure. Given the high number of acquired (indicatively, a mean rate of 2500 counts s^{-1}) photons, and the extremely accurate time tagging guaranteed by Iqueye, we feel confident to say that the Iqueye light curve shown in Fig. 1 is the best available so far in visible light. The total duration of the main peak is approximately 22 ms [full width at half-maximum (FWHM)], with a central shallower feature suggesting the superposition of at least two peaks, as indicated also by the steeper slope of the ascending branch with respect to the descending one (0.062 ± 0.004 versus -0.046 ± 0.005 in units of normalized flux per phase unit) and already found by De Plaa et al. (2003) from X-ray data. Therefore, we have fitted the broad central peak with two Gaussian components separated by 0.29 (± 0.02) in phase, the leading one approximately 1.02 times higher than the second one, and with a FWHM of 13.3 ± 0.2 and 15.5 ± 0.2 ms, respectively.

4 DISCUSSION OF THE BRAKING INDEX AND AGE

In commonly assumed models for pulsar spin-down, a braking index n and a characteristic age τ_c are defined (Livingstone et al. 2007) by

$$\dot{\nu} = -K\nu^n, \qquad n = \frac{\nu\ddot{\nu}}{\dot{\nu}^2}, \qquad \tau_c = \frac{\nu}{2\dot{\nu}}, \tag{2}$$

where ν is the pulse frequency, $\dot{\nu}$ and $\ddot{\nu}$ are the first and second frequency derivatives, respectively, and K is a constant. The braking index provides insight into the physics of the pulsar mechanism. Indeed, the actual value of the braking index is strictly related to the pulsar spin-down mechanism. It is well known (Manchester & Taylor 1977) that for magnetic dipole emission, as well as for the aligned rotator model of Goldreich & Julian (1969), $n = 3$. Different values of n would correspond to different processes of rotational energy loss and, in particular, values lower than 3 indicate that an additional torque is contributing to the spin-down. It should be noted that the value of n also affects the determination of the pulsar age, with $n < 3$ providing consistently larger values than those predicted by the characteristic age. Among the additional spin-down mechanisms, the distortion of the magnetic dipole geometry, a time variable magnetic field, a change with time of the inclination angle between rotation and magnetic axes and/or the presence of particles/currents in the magnetosphere have been suggested (Ghosh 2007; Livingstone et al. 2007). As for the Crab pulsar, in the case of PSR B0540−69 the existence of a synchrotron-emitting nebula around the pulsar provides independent evidence for a particle wind originating from the pulsar magnetosphere, whose plasma may then contribute an additional spin-down torque (as suggested also by Boyd et al. 1995). However, precisely determining what physical mechanism is responsible for the observed braking index of PSR B0540−69 and pulsars in general remains a completely open question. Unfortunately, the measurement of the braking index n is a difficult task, and only the youngest pulsars (typical ages less than 2 kyr) possess all needed qualities, in particular rapid spin-down and small relatively infrequent glitches. As an example, a braking index $n = 2.51 \pm 0.01$ has been measured for the Crab pulsar. PSR B0540−69 bears many similarities to the Crab pulsar, like period and magnetic-field strength (50 versus 30 ms, 5×10^{12} versus 4×10^{12} G; see Campana et al. 2008), but its much larger distance prevents regular radio observations, and conflicting values of n are reported in the literature. Livingstone, Kaspi & Gavriil (2005) concluded, by a careful analysis of all X-ray data obtained using 7.6 yr of data from the *Rossi X-Ray Timing Explorer*, that the best estimate for the braking index is $n = 2.140 \pm 0.009$. The optical data available until our observations provided the following values: Manchester & Peterson (1989), $n = 2.01 \pm 0.02$; Gouiffes et al. (1992), $n = 2.04 \pm 0.02$; and Boyd et al. (1995), $n = 2.28 \pm 0.02$. We calculated the first and second frequency derivatives adding the frequency values measured with Iqueye in 2009 January and December to the previously published data sets. The frequency values considered for our analysis are summarized in Table 4. We have taken into account only measured, i.e. not interpolated, values, covering the entire spectrum from radio to X-ray at different dates. These values have been fitted with a second-order polynomial (Fig. 2), using least-squares regression, in the assumption of none or very small and infrequent glitches:

$$\nu(t) = \nu(t_0) + \dot{\nu}(t - t_0) + \frac{1}{2}\ddot{\nu}(t - t_0)^2. \tag{3}$$

The coefficients of the best-fitting parabola, where t_0 is the value of the last date of observations, are reported in Table 5.

With the so determined values of t_0, ν_0, $\dot{\nu}_0$ and $\ddot{\nu}_0$, the resulting value for the braking index is $n = 2.087 \pm 0.007$, and the characteristic age is $\tau = 1677.5$ yr. Our result is consistent within 3 combined σs with the value given by Livingstone et al. (2005) and it confirms

Table 4. Frequencies used for the calculation of the braking index. Values are taken from the corresponding papers indicated in the last column and ordered by MJD.

MJD	Frequency (Hz)	Band	Ref.
44186.91740	19.916 875 32	X	Seward et al. (1984)
45940.86590	19.888 115 20	VIS	Middleditch & Pennypacker (1985)
46111.07682	19.885 331 33	VIS	Middleditch & Pennypacker (1985)
47860.0000	19.856 747 51	Radio	Manchester et al. (1993)
47915.0000	19.855 849 39	Radio	Manchester et al. (1993)
48825.8000	19.840 996 63	Radio	Manchester et al. (1993)
49225.25570	19.834 496 50	*HST* (UV+VIS)	Boyd et al. (1995)
51421.62400	19.798 800 10	X	Kaaret et al. (2001)
52857.86600	19.775 530 00	X	Johnston et al. (2004)
53761.76200	19.760 922 60	X	Campana et al. (2008)
53843.56100	19.759 595 20	X	Campana et al. (2008)
54849.21665	19.743 346 57	VIS (Iqueye)	This work
54851.16190	19.743 329 88	VIS (Iqueye)	This work
55179.31111	19.738 056 33	VIS (Iqueye)	This work
55180.11250	19.738 023 95	VIS (Iqueye)	This work
55181.06944	19.738 008 90	VIS (Iqueye)	This work
55183.10417	19.737 977 09	VIS (Iqueye)	This work

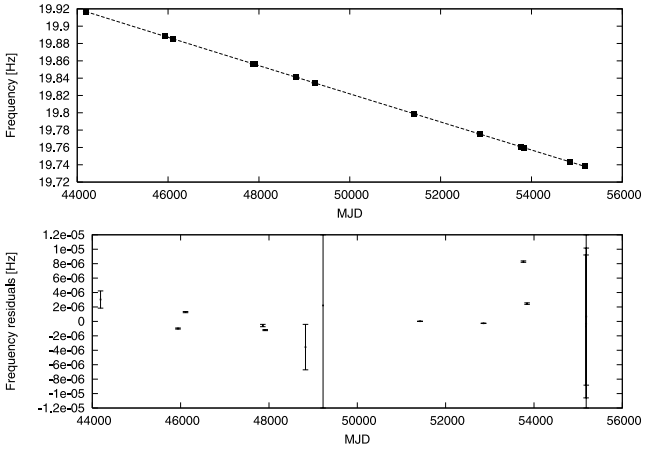

Figure 2. Fit over the data shown in Table 4.

Table 5. The coefficients of the second-order polynomial used for the fit.

	Value	Error
t_0 (MJD)	55183.1042	
ν_0 (Hz)	19.737 9764	$\pm 1 \times 10^{-6}$
$\dot{\nu}_0$ (Hz s^{-1})	$-1.865\,60 \times 10^{-10}$	$\pm 5 \times 10^{-15}$
$\ddot{\nu}_0$ (Hz s^{-2})	3.66×10^{-21}	$\pm 1 \times 10^{-23}$

that the value of the braking index for this pulsar is definitely lower than 3.

5 CONCLUSIONS

We have observed the LMC B0540−69 pulsar with Iqueye, a novel extremely high time resolution photometer, obtaining data of unprecedented timing accuracy. The data provide the most detailed optical light curve available so far for this pulsar, extending to 27 years the time spanned by X-ray, optical and radio data and allowing a refined determination of the first and second derivatives of the pulsar spin rate. The resulting value of the braking index, $n = 2.087$, provides increasingly consistent evidence that the braking index of the LMC pulsar B0540−69 is slightly higher than $n = 2$, and definitely smaller than the magnetic dipole value $n = 3$, in agreement with the findings for all young pulsars for which it has been possible to perform such measurement (with the possible exception of PSR J1119−6127 for which it has been measured as $n = 2.91$; Camilo et al. 2000).

ACKNOWLEDGMENTS

We wish to acknowledge the support given by ESO and the personnel at La Silla Observatory for the perfect operation of Iqueye at NTT. This work has been supported by the University of Padova, the Italian Ministry of Research and University MIUR, the Italian Institute of Astrophysics INAF, the Fondazione Cariparo Padova, the GALILEO GNSS Supervising Authority through the Harrison Project. Thanks are due to R. Mignani for the kind help with the finding chart and useful suggestions. We wish also to thank the referee who pointed out an error in our calculation of the error of the period, and greatly helped to improve the content.

REFERENCES

Barbieri C. et al., 2009, Proc. SPIE, 7355, 25
Barbieri C. et al., 2010, Proc. SPIE, 7681, 4
Boyd P. T. et al., 1995, ApJ, 448, 365
Camilo F., Kaspi V. M., Lyne A. G., Manchester R. N., Bell J. F., D'Amico N., McKay N. P. F., Crawford F., 2000, ApJ, 541, 367
Campana R., Mineo T., De Rosa A., Massaro E., Dean A. J., Bassani L., 2008, MNRAS, 389, 691
Deeter J. E., Nagase F., Boynton P. E., 1999, ApJ, 512, 300
De Luca A., Mignani R. P., Caraveo P. A., Bignami G. F., 2007, ApJ, 667, L77
De Plaa J., Kuiper L., Hermsen W., 2003, A&A, 400, 1013
Dravins D. et al., 2005, arXiv:astro-ph/0511027v1, 11027
Ghosh P., 2007, Rotation and accretion powered pulsars. World Scientific Publishing, Singapore
Goldereich P., Julian W., 1969, ApJ, 157, 869
Gouiffes C., Finley J. P., Ögelman H., 1992, ApJ, 394, 581
Hanbury Brown R., 1974, The intensity interferometer. Taylor & Francis, London
Hobbs G. B., Edwards R. T., Manchester R. N., 2006, MNRAS, 369, 665

Johnston S., Romani R. W., Marshall F. E., Zhang W., 2004, MNRAS, 355, 31
Kaaret P. et al., 2001, ApJ, 546, 1159
Larsson S., 1996, A&A, 117, 197
Leahy D. A., 1987, A&A, 180, 275
Leahy D. A., Elsner R. F., Weisskopf M. C., 1983, ApJ, 272, 256
Livingstone M. A., Kaspi V. M., Gavriil F. P., 2005, ApJ, 633, 1095
Livingstone M. A., Kaspi V. M., Gavriil F. P., Manchester R. N., Gotthelf E. V. G., Kuiper L., 2007, Astrophys. Space Sci. Lett., 308, 317
Manchester R. N., Peterson B. A., 1989, ApJ, 342, L23
Manchester R. N., Taylor J. H., 1977, Pulsars. Freeman, San Francisco
Manchester R. N., Mar D. P., Lyne A. G., Kaspi V. M., Johnston S., 1993, ApJ, 403, L29
Middleditch J., Pennypacker C. R., 1985, Nat, 313, 659
Middleditch J., Pennypacker C. R., Burns M. S., 1987, ApJ, 315, 142
Mignani R. P., Mereghetti S., Gouiffes C., Caraveo P. A., 1998, The Messenger, 94, 25
Mignani R. P., Sartori A., De Luca A., Rudak B., Slowikowska A., Kanbach G., Caraveo P. A., 2010, A&A, 515, 110
Mineo T., Cusumano G., Massaro E., Nicastro L., Parmar A. N., Sacco B., 1999, A&A, 348, 519
Naletto G. et al., 2009, A&A, 508, 531
Naletto G. et al., 2010, Proc. SPIE, 7735, 138
Serafimovich N. I., Shibanov Yu. A., Lundqvist P., Sollerman J., 2004, A&A, 425, 1041
Seward F. D., Harnden F. R., Jr, Helfand D. J., 1984, ApJ, 287, L19
Shearer A., Redfern M., Pedersen H., Rowold T., O'Kane P., Butler R., O'Byrne C., Cullum M., 1994, ApJ, 423, L51
Skrutslie M. F. et al., 2006, AJ, 131, 1163
Standish E. M., 1998, JPL Planetary and Lunar Ephemerides, JPL IOM, 312.F-98-048
Ulmer M. P., Park S., Finley J. P., Middleditch J., Codes M. J., 1999, Astrophys. Lett. Commun., 38, 29

This paper has been typeset from a TEX/LATEX file prepared by the author.